

## MODE II CHARACTERIZATION OF CORTICAL BONE TISSUE USING THE ELS TEST

F.A.M. Pereira<sup>1</sup>, J.J.L. Morais<sup>1</sup>, N. Dourado<sup>1</sup>, M.F.S.F. de Moura<sup>2</sup>, M.I.R. Dias<sup>3</sup>

<sup>1</sup> CITAB/UTAD, Departamento de Engenharias, Quinta de Prados, 5001-801  
Vila Real, Portugal

<sup>2</sup> Faculdade de Engenharia da Universidade do Porto, Departamento de Engenharia Mecânica, Rua Dr. Roberto Frias,  
4200-465 Porto, Portugal

<sup>3</sup> UTAD, Departamento de Ciências Veterinárias, Quinta de Prados, 5001-801  
Vila Real, Portugal

### ABSTRACT

A miniaturized testing device of the end load split (ELS) test was conceived to evaluate fracture energy release rate under pure mode II loading of young bovine cortical bone tissue. Since crack length is not possible to monitor during propagation, classical methods cannot be applied to determine fracture energy in this material. Hence, an equivalent crack technique, which does not necessitate the crack length surveillance, was used to assess the equivalent crack extent. The applied data reduction scheme is based on the specimen compliance, beam theory and crack equivalent concept, providing the assessment of the energy release rate. The method was fully validated through a numerical analysis, by means cohesive zone modeling.

**KEYWORDS:** Bone, Fracture characterization, Mode II, End loaded split test.

### 1. INTRODUCTION

Bone fracture is an important research topic as it can contribute to understand the essentials of bone failure induced by age, drugs, disease and immoderate exercise. Effectively, fracture mechanics measurements can be regarded as a valuable way to characterize toughness in bone, thus providing a quantitative evaluation of its fracture resistance. Therefore, the definition of valuable testing methods to assess fracture properties of bone turns crucial. Though, classical fracture procedures normally performed in other materials require special adaptations due to bone characteristics. In effect, bone can be viewed as a natural composite material constituted essentially by an inorganic (mineral) phase (i.e., the hydroxyapatite), collagen fibers and water. These materials are organized in a microstructure highly anisotropic and heterogeneous. This microstructure is responsible for the development of a non-negligible fracture process zone (FPZ), which means that linear elastic fracture mechanics (LEFM) theory is not valid. In such case, non-linear fracture mechanics approaches, as is the case of cohesive zone modelling, should be considered. An additional difficulty is related to limitations on specimen dimensions that are possible to be harvested from bone. These aspects hinder the definition of adequate tests to analyze fracture characteristics of bone.

In the literature there are only few works dedicated to mode II fracture in bone [1, 2, 3]. The fundamental reasons are related to experimental difficulties, namely

the definition of an appropriate test method. However, fracture characterization under mode II acquires special relevancy for different reasons. Effectively, fractures can occur under pure shear loading, as is the case of twisting or torsion efforts during normal activities [4]. De Moura et al. (2010) [5] have recently performed detailed numerical analyses using cohesive zone modeling on the application of the end loaded split (ELS) and end notched flexure (ENF) tests to pure mode II fracture characterization of bone. Considering typical ranges of bone properties the authors concluded that both tests can be used for this objective, with a judicious selection of specimens' dimensions. However, the authors realized that the ELS test provides a longer extent with self-similar crack propagation, i.e., without spurious effects affecting the free development of FPZ. As a consequence of this statement the ELS test is used in the present work to characterize fracture behavior of cortical bovine bone under pure mode II loading. With this aim, a miniaturized testing device was designed in order to account for bone specificities, namely the available specimen size. An equivalent crack length method based on beam theory and specimen compliance was used to overcome the difficulties inherent to crack monitoring during its growth. The data reduction scheme provides the attainment of the R-curve, which allows determining the extent of the FPZ and the critical fracture energy from its plateau. The method was numerically validated by means of cohesive zone modeling, which permits simulating damage initiation and growth. The data reduction method was

subsequently applied with success to experimental results in order to evaluate mode II bone toughness. The main conclusion is that the proposed test (ELS) and data reduction scheme provide a simple, expedite and adequate methodology to evaluate mode II fracture characteristics of bone.

## 2. EXPERIMENTS

Ten specimens were prepared from fresh bovine femora of young animals (aged about 8 months) within one day post-mortem. During the specimens preparation the endosteal and periosteal tissues were removed. Specimens were preserved with physiological saline at all steps of the machining process and frozen at  $-20^{\circ}\text{C}$  for storage. The initial crack length  $a_0$  is constituted by a notch (0.3 mm thick) performed with a circular saw, and a small crack (0.25 mm length) executed with a sharp blade. This process usually reproduces natural cracks in a realistic way. This is an important issue since blunt pre-cracks reflect on unrealistic increase of fracture energy at crack starting advance [6]. Nevertheless, as will be discussed later, the used data reduction scheme allows overcoming any imprecision on the execution of the pre-crack. As observed in Fig. 1, specimens were conceived in order to provide propagation in the TL fracture system (i.e., the normal to the crack plane is the tangential direction of mid-diaphysis and the crack propagation direction is the longitudinal direction of mid-diaphysis). Prior to the pre-crack execution the longitudinal modulus ( $E_L$ ) was determined for each specimen before introducing the pre-crack, by means of three-point bending test. Since the experimental praxis during the ELS tests revealed that crack frequently deviates from its initial plane ( $z = 0$  in Fig. 2), two slight longitudinal grooves have been machined in each lateral side of the specimen to diminish the width ( $b$  instead of  $B$  in Fig. 2) of the ligament area, thus compelling crack

advance to occur along the L-axis. Previous simulations [5] and preliminary fracture tests allowed the definition of adequate specimen nominal dimensions:  $L_1 = 60$ ,  $L = 50$ ,  $d = 3$ ,  $a_0 = 20$ ,  $2h = 6$ ,  $b = 2.3$ ,  $B = 3.3$  and  $t = 1$  (dimensions in mm).

Fracture tests were performed under displacement control (0.5 mm/min) using a servo-electrical material testing system (MicroTester INSTRON 5848), using a 2 kN load-cell, for an acquisition frequency of 5 Hz. During the test, the applied load ( $P$ ) and displacement ( $\delta$ ) were registered. As observed in Fig. 3 the fixture testing device includes a linear guidance system which allows horizontal translation of the clamping grip during the loading process. This solution avoids tensile stress development along the longitudinal direction.

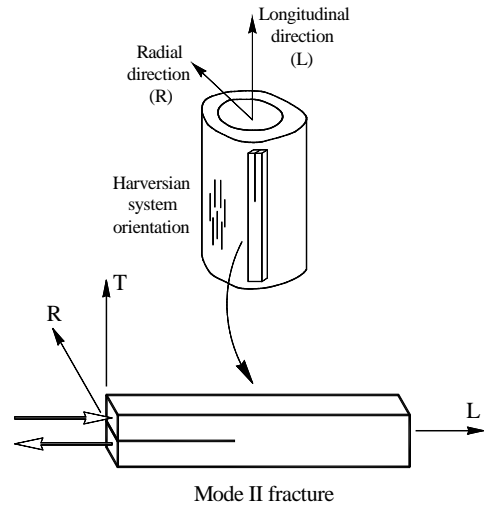


Figure 1. Schematic diagram of a bone femur showing the location where samples can be harvested.

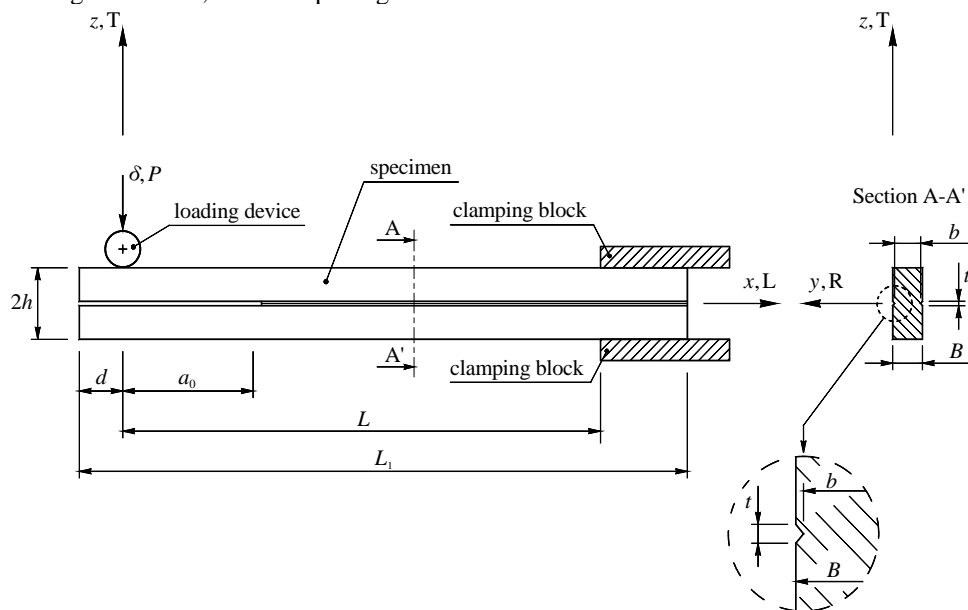


Figure 2. Schematic representation of the ELS test.

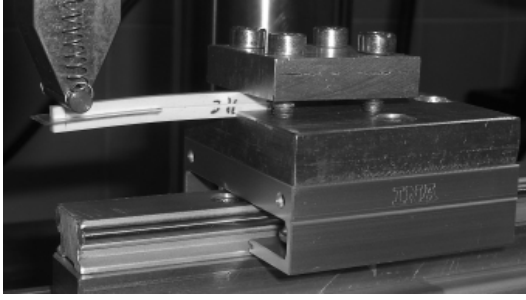


Figure 3. Testing setup.

Two thin Teflon® films with a pellicle of lubricator between them were introduced in the pre-crack region (Fig. 3) to reduce the friction effects [9]. One crucial aspect of this test is associated to the clamping conditions. In a recent numerical study [5] the effect of tightening was thoroughly analyzed. It was verified that a tightening of 0.1 mm provides satisfactory measurements of mode II toughness ( $G_{IIc}$ ) without overcoming compressive strength of bone.

Fig. 4 shows the crack detail during propagation. Sliding at the notch tip (see detail in Fig. 4) clearly demonstrates the existence of a pure mode II loading. On the other hand, it is evident that the position of the crack tip is not undoubtedly identified with the necessary accuracy. As a result, the application of classical data reduction schemes based on crack length ( $a$ ) monitoring during propagation can lead to miscalculations of fracture energy, due to errors committed on the crack length measurements. To overcome this drawback an equivalent crack length based method is presented in the next section.

### 3. CRACK EQUIVALENT BASED METHOD

Mode II fracture energy is classically measured through compliance calibration method (CCM) or by means of corrected beam theory (CBT). Both methods require crack length monitoring, which is not easy to accomplish with the required accuracy, as discussed in the previous section (Fig. 4). To obviate this disadvantage a crack equivalent method based on current specimen compliance and beam theory is adopted. The equation of compliance as a function of crack length using the Timoshenko beam theory is

$$C - \frac{3a^3}{2Bh^3E_L} = \frac{L^3}{2Bh^3E_L} + \frac{3L}{5BhG_{LT}} \quad (1)$$

In the ELS test the clamping conditions are never perfect. In order to account for this effect, an effective specimen length ( $L_{ef}$ ) which, in fact, is the theoretical length that specimen should present in order to satisfy Eq. (1), should be considered. This parameter ( $L_{ef}$ ) can be estimated using the initial (elastic) response of experimental test (i.e.,  $a_0$  and  $C_0$ ) in Eq. (1),

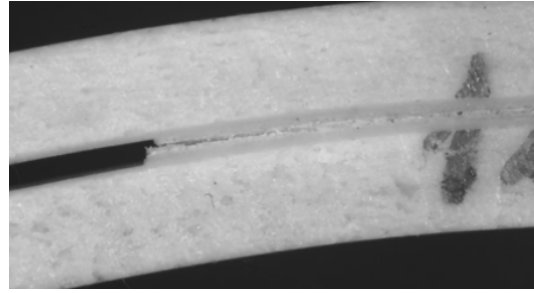


Figure 4. Specimen detail showing the relative displacement at the crack notch.

$$C_0 - \frac{3a_0^3}{2Bh^3E_L} = \frac{L_{ef}^3}{2Bh^3E_L} + \frac{3L_{ef}}{5BhG_{LR}} \quad (2)$$

Combining Eqs. (1) and (2) the equivalent crack length (instead of  $a$ ) during propagation becomes

$$a_e = \left[ (C - C_0) \frac{2Bh^3E_L}{3} + a_0^3 \right]^{1/3} \quad (3)$$

which do not depend on parameter  $L_{ef}$ . The strain energy release rate in mode II ( $G_{II}$ ) can now be obtained from Eqs. (3) and Irwin-Kies equation. It should be noted that due to the presence of the longitudinal grooves (Fig. 2) the width of the ligament section is  $b$ , instead of  $B$ . Therefore,

$$G_{II} = \frac{9P^2a_e^2}{4bBh^3E_L} \quad (4)$$

Following this methodology the mode II  $R$ -curve is obtained as a function of  $a_e$ , and the critical fracture energy  $G_{IIc}$  is captured from its plateau. The method only requires the previous measurement of  $E_L$  as well as the load-displacement data obtained during the experimental test. Hence, the problem associated to crack length monitoring is surmounted, since the crack is a calculated parameter instead of a measured one. Additionally, this procedure allows accounting for the fracture process zone (FPZ) development. In fact, quasi-brittle materials like bone are characterized by a non-negligible FPZ which must be accounted for, since its presence affects fracture behavior. This is achieved by means of the proposed data reduction scheme, seeing that the FPZ influences specimen compliance which is used to get the  $R$ -curve.

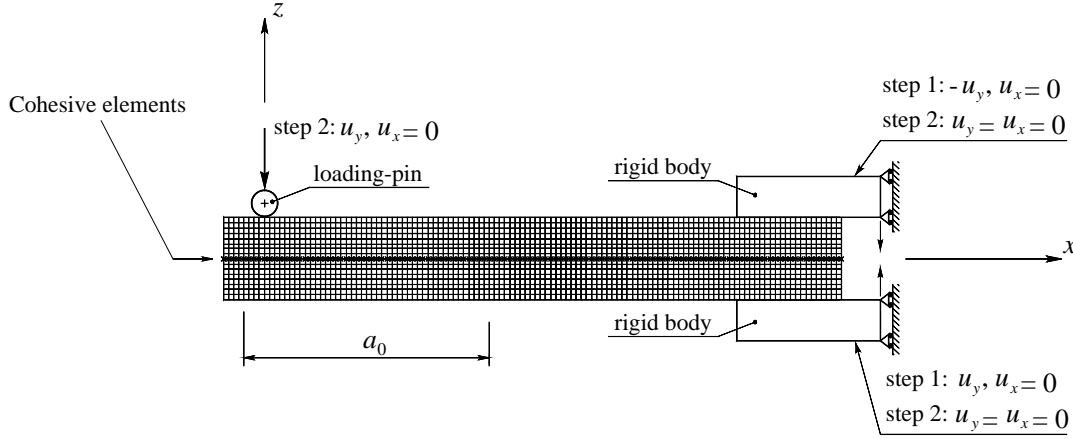


Figure 5. Finite element mesh used in the numerical simulations. Diagonal crosses at the mid-thickness represent cohesive elements.

#### 4. MODEL VALIDATION

In order to validate the proposed data reduction scheme (section 3) a numerical analysis including cohesive zone modeling was performed. A two-dimensional plane stress analysis involving 7680 8-node solid elements (width  $B$ ), and 240 6-node cohesive elements (width  $b$ ) allowing to simulate damage onset and propagation, was performed (Fig. 5). Following this strategy, the presence of the longitudinal grooves in the specimen is taken into account, given that the fracture section presents a width  $b$  instead of  $B$  (Fig. 2). Opened cohesive elements were considered in the pre-crack region in order to avoid interpenetration. These opened elements transmit normal compressive stresses and allow a free sliding between the crack surfaces. Since thin lubricated Teflon® films were introduced at the pre-crack, friction effects were neglected. The loading cylinder (Fig. 3) was simulated as a rigid body (Fig. 5) and contact conditions were considered to avoid interpenetration. Two rectangle rigid blocks were used to impose clamping conditions (step 1 in Fig. 5) by tightening the specimen (0.1 mm) prior to the load application, considering a friction coefficient of 0.25. Fracture was induced in the TL system imposing a vertical displacement (step 2:  $u_y$  in Fig. 5) to the loading-pin. Typical elastic properties of bovine cortical bone (Table 1) were used in the numerical model. A mixed-mode cohesive damage model was incorporated in the numerical analysis. A linear softening relationship between stresses and relative displacements (Fig. 6) is assumed to simulate a gradual material degradation during the loading process. The cohesive zone model establishes a relationship between stresses and relative displacements. In the initial linear region stresses are obtained from the product between the interfacial stiffness and relative displacements. Once the local strength ( $\sigma_{u,i}$ ,  $i=I, II$ ) is attained the initial interface stiffness is gradually reduced leading to a linear decrease of stresses. In pure mode model, the ultimate relative displacement  $w_{u,i}$  ( $i=I, II$ ) is defined equating the area circumscribed by the triangle to  $G_{ic}$  ( $i=I, II$ ).

Mixed-mode damage model is an extension of pure mode model. In this case, a quadratic stress criterion is utilized to simulate damage onset

$$\left(\frac{\sigma_I}{\sigma_{u,I}}\right)^2 + \left(\frac{\sigma_{II}}{\sigma_{u,II}}\right)^2 = 1 \quad \text{if } \sigma_I \geq 0 \quad (5)$$

$$\sigma_{II} = \sigma_{u,II} \quad \text{if } \sigma_I \leq 0$$

where  $\sigma_i$  represent the stresses in each mode and  $\sigma_{u,i}$  the respective local strengths. Crack propagation was simulated by a linear energy criterion

$$\frac{G_I}{G_{Ic}} + \frac{G_{II}}{G_{IIc}} = 1 \quad (6)$$

From Fig. 6 it is shown that the area of triangle  $0-\sigma_{um,i}-w_{um,i}$  corresponds to the energy released in each mode ( $G_i$ ,  $i=I, II$ ) during mixed-mode loading. Eqs. (5) and (6) can be written exclusively as a function of relative displacements, considering the relation between stresses/relative displacements as well as the one involving energies/relative displacements.

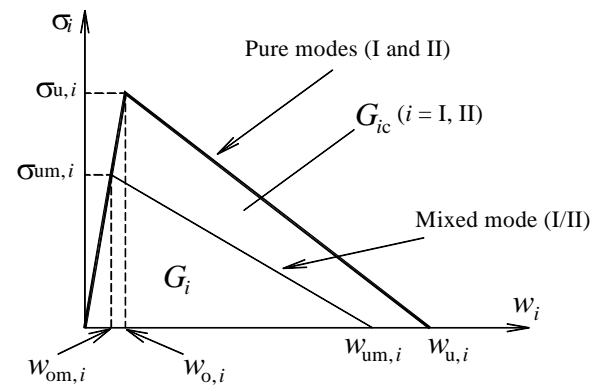


Figure 6. Sketch of pure (I or II) and mixed (I+II)

bilinear cohesive model.

This procedure allows defining the equivalent critical mixed-mode displacements corresponding to damage onset ( $w_{om} = \sqrt{w_{om,I}^2 + w_{om,II}^2}$ ) and crack growth

( $w_{um} = \sqrt{w_{um,I}^2 + w_{um,II}^2}$ ) under mixed-mode loading.

These quantities are used to determine a damage parameter whose evolution is responsible for stress and stiffness decrease during loading. The cohesive zone model is detailed in de [9].

Typical values of local strength  $\sigma_{u,II} = 51.6$  MPa [4] and mode II toughness  $G_{IIc} = 2.43$  N/mm [10] were used in the numerical analysis. Fig. 7 shows the plotting of the  $R$ -curve normalized by the inputted toughness  $G_{IIc}$  in the cohesive model. As can be concluded, the inputted  $G_{IIc}$  is well captured in the plateau of the  $R$ -curve, which demonstrates that the proposed data reduction scheme (section 3) is valid to evaluate fracture toughness in bone. Consequently, the method will be applied in the next section to experimental data.

## 5. RESULTS AND DISCUSSION

Fig. 8 presents a typical load-displacement curve obtained in the experiments as well as the respective  $R$ -curve determined by means of the procedure described in section 3. The raise in the energy release rate observed in the ascending part of the  $R$ -curve reflects the FPZ development. This phenomenon induces material softening which leads to stiffness reduction and gradual failure. When the FPZ is completely developed a self-similar crack growth takes place, i.e., the crack propagates with a constant FPZ size ahead of its tip. This leads to a plateau on the  $R$ -curve which defines the material fracture toughness under pure mode II. An additional advantage of this procedure is related to the fact that  $R$ -curves allow measurement of critical fracture energy during self-similar crack growth, independently of spurious problems related to pre-crack fabrication. Effectively, a blunt pre-crack induces an artificial initial increase of fracture energy followed by a plateau that provides the evaluation of material toughness [6].

A resume of the experimental results is presented in Table 2. The elastic longitudinal modulus ( $E_L$ ) was measured for each specimen, since it is fundamental to calculate the fracture energy (Eq. 4). The values of  $G_{IIc}$

In order to verify if the proposed data reduction scheme is able to reproduce accurately the material fracture energy, the specimen whose results are presented in Fig. 8 was numerically simulated. The value given by the plateau ( $G_{IIc} = 2.64$  N/mm) was inputted in the numerical model and the resulting load-displacement curve was compared with the experimental one. Fig. 9(a) shows the good agreement obtained when a local strength of  $\sigma_{u,II} = 65$  MPa was used. Additionally, it was observed that a cohesive zone with a constant length of approximately 3.0 mm (Fig. 9 b) reproducing the FPZ is obtained during propagation, for a certain extent of equivalent crack growth. After that, confinement of the cohesive zone takes place thus inducing a spurious increase of measured fracture energy. This means that the proposed geometry is adequate to bone fracture characterization under mode II loading since self-similar crack growth conditions arise for a given extent of crack propagation.

Table 2. Resume of experimental results.

Specimen	$E_L$ (GPa)	$G_{IIc}$ (N/mm)
1	18.2	2.55
2	19.2	2.65
3	20.3	2.45
4	18.8	2.90
5	19.1	2.38
6	19.9	2.64
7	17.2	2.85
8	15.7	2.75
9	17.8	2.95
10	17.1	2.40
Average	18.3	2.65
CoV (%)	7.7	7.8

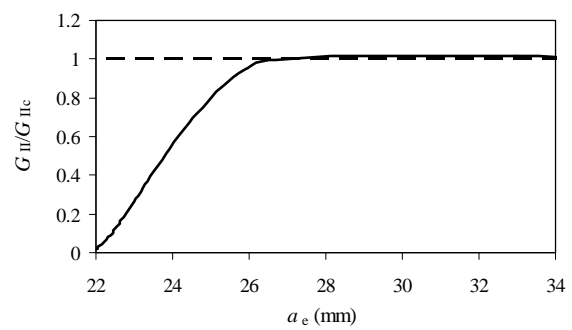


Figure 7. Numerical  $R$ -curve of the ELS test.

Table 1. Elastic properties of bovine cortical bone [6, 11].

$E_L$ (GPa)	$E_T$ (GPa)	$G_{LT}$ (GPa)	$\nu_{LT}$
19.94	11.7	4.1	0.36

were captured from the plateau of the  $R$ -curves. An average value of  $G_{IIc} = 2.65$  N/mm was obtained with a coefficient of variation of 7.8%, which can be considered reasonable for a biological material.

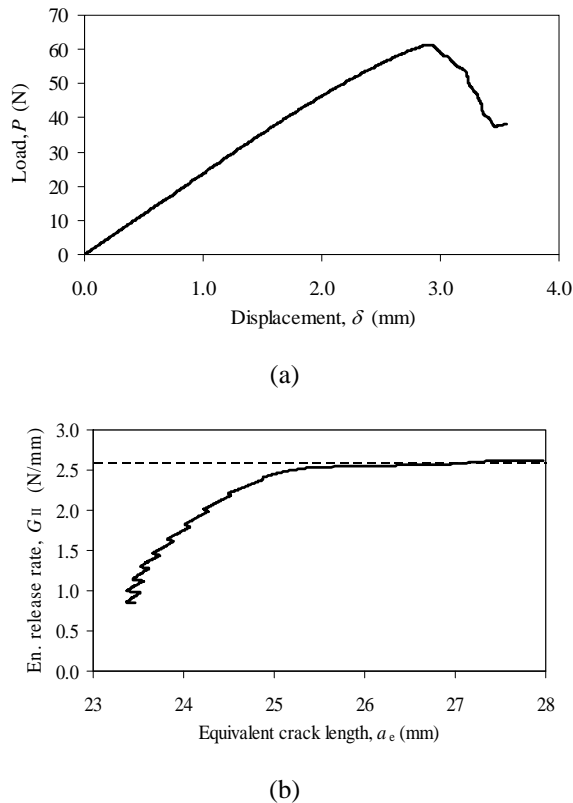


Figure 8. Typical load-displacement curve (a) and corresponding R-curve (b).

## 6. CONCLUSIONS

In this work, the applicability of the ELS test to mode II fracture characterization of bone was performed. Experimental tests were executed considering a miniaturized version of the classical setup used in this test. A data reduction scheme based on crack equivalent concept was applied in order to overcome the difficulties associated to crack measurement during its growth. The method was numerically validated by means of a mixed-mode I+II cohesive zone model. After that the data reduction scheme was applied to the experimental data to get the Resistance-curve that allows a clear definition of fracture energy from its plateau under mode II loading of bone. It was concluded that the ELS test using adequate specimen dimensions is appropriate to determine mode II fracture toughness in bone.

## ACKNOWLEDGEMENTS

The authors acknowledge the Portuguese Foundation for Science and Technology (FCT) for the conceded financial support through the research project PDTC/EME/PME/119093/2010.

## REFERENCES

[1] Norman, T.L., Nivargikar, V., Burr, D.B., 1996. Resistance to crack growth in human cortical bone

is greater in shear than in tension. *Journal of Biomechanics* 29, 1023–1031.

[2] Zimmermann, E.A., Launey, M.E., Barth, H.D., Ritchie, R.O., 2009. Mixed-mode fracture of human cortical bone. *Biomaterials* 30, 877–884.

[3] Zimmermann, E.A., Launey, M.E., Ritchie, R.O., 2010. The significance of crack-resistance curves to the mixed-mode fracture toughness of human cortical bone. *Biomaterials* 31, 5297–5305.

[4] Turner, C.H., Wang, T., Burr, D.B., 2001. Shear strength and fatigue properties of human cortical bone determined from pure shear tests. *Calcified Tissue International* 69, 373–378.

[5] de Moura, M.F.S.F., Dourado, N., Morais, J.J.L., Pereira, F.A.M., 2010b. Numerical analysis of the ENF and ELS tests applied to mode II fracture characterization of cortical bone tissue. *Fatigue & Fracture of Engineering Materials & Structures* 34, 149–158.

[6] Morais J.J.L., de Moura M.F.S.F., Pereira F.A.M., Xavier J., Dourado N., Dias M.I.R., Azevedo J.M.T., 2010. The double cantilever beam test applied to mode I fracture characterization of cortical bone tissue. *Journal of Thomechanical Behavior of Biomedical Materials* 3:446–453.

[7] de Moura, M.F.S.F., Silva, M.A.L., Morais, J.J.L., de Morais, A.B., Lousada, J.J.L., 2009. Data reduction scheme for measuring  $G_{IIc}$  of wood in End-Notched Flexure (ENF) tests. *Holzforschung* 63, 99–106.

[8] Wang, Y., Williams, J.G., 1992. Corrections for mode II fracture toughness specimens of composite materials. *Composites Science and Technology* 43, 251–256.

[9] de Moura, M.F.S.F., Silva, M.A.L., de Morais, A.B., Morais, J.J.L., 2006. Equivalent crack based mode II fracture characterization of wood. *Engineering Fracture Mechanics* 73, 978–993.

[10] Feng, Z., Rho, J., Han, S., Ziv, I., 2000. Orientation and loading condition dependence of fracture toughness in cortical bone. *Materials Science and Engineering C* 11, 41–46.

[11] Martin, R.B., Burr, D.B., Sharkey, N.A., 1998. *Skeletal Tissue Mechanics*, ISBN 0-387-98474-7. Springer-Verlag, New York.